Compact wavelength monitoring by lateral outcoupling in wedged photonic crystal multimode waveguides

Emilie Viasnoff-Schwoob, Claude Weisbuch, Henri Benisty, Cornélia Cuisin, Estelle Derouin, Olivier Drisse, Guang Hua Duan, Lionel Legouezigou, Odile Legouezigou, Frédéric Pommereau, et al.

Compact wavelength monitoring by lateral outcoupling in wedged photonic crystal multimode waveguides

E. Viasnoff-Schwoob and C. Weisbuch
Laboratoire PMC, Ecole Polytechnique, 91128 Palaiseau, France

H. Benisty[a)]
Laboratoire Charles Fabry de l'Institut d'Optique, Bat 503, 91403 Orsay cedex, France

C. Cuisin, E. Derouin, O. Drisse, G-H. Duan, L. Legouézigou, O. Legouézigou, and F. Pommereau
OPTO+, Alcatel Research and Innovation, Route de Nozay, 91460 Marcoussis, France

S. Golka, H. Heidrich, H. J. Hensel, and K. Janiak
Fraunhofer Institute for Telecommunications, Heinrich-Hertz-Institut, Einsteinufer 37, 10587 Berlin, Germany

(Received 9 August 2004; accepted 18 January 2005; published online 3 March 2005)

A device concept for laterally extracting selected wavelengths from an optical signal traveling along a waveguide, for operation in metropolitan area networks, is presented. The signal on the fundamental mode of a multimode photonic crystal waveguide is coupled to a higher-order mode, at a center frequency that spatially depends on the slowly varying guide parameters. The device is compact, intrinsically fault tolerant, and can split any desired fraction of the signal for monitoring purpose. Characterizations by the internal light source technique validate the optical concept whereas an integrated device with four photodiodes qualifies its potential with respect to real-world applications. © *2005 American Institute of Physics*. [DOI: 10.1063/1.1879105]

Wavelength monitoring is one of the key functions needed at nodes of wavelength division multiplexing metropolitan optical networks. Monolithic solutions on InP-based heterostructure, such as standard one-dimensional Bragg reflectors[1] phasar type solutions,[2] micromechanically tuned vertical Fabry-Pérot cavities,[3] and microring resonator filters,[4] have been tackled in classical integrated optics. Their footprints are still in the 1 mm^2 range and none of these solutions have a practical, cost-efficient geometry for monitoring purpose, which would transmit most of the signal.

Meanwhile, matured planar photonic crystal technology makes optical integrated circuits based on these two-dimensional (2D) structures increasingly attractive. Compact and fault-tolerant coupler,[5] power lasers,[6] coupled-cavity lasers[7] are some examples of components using the specific functionalities, such as confinement and diffraction, provided by photonic crystals. Among all available devices, multimode photonic crystal channel waveguides (PXCW) are known to exhibit specific anticrossings between guided modes *of different orders*. This mode coupling occurs through the corrugation of the boundary of the PXCW and is nothing but a Bragg diffraction. The impact of this so-called mini-stop-band (MSB) on the transmission has been detailed.[8,9] In this letter, we propose a use of mode-coupling in PXCW: combined with a slow spatial variation of guide parameters [Figs. 1(a) and 1(b)], it lends itself to wavelength monitoring in a very compact and simple way, namely detection by integrated photodiodes located aside the guide.

As seen on Figs. 1(a) and 1(b), the principle takes advantage of a multimode PXCW with a slight wedge (smooth or "staircased"), resulting in a shifting spectral position of the MSB [Fig. 1(c)]. The guide couples its fundamental (quasirefractive) mode to a higher-order mode only inside the local MSB's narrow wavelength window. Outside the MSB, the fundamental mode is unaffected. Hence, when a transverse electric (TE) signal enters the device, its spectral components are unaffected in all sections but the critical, cou-

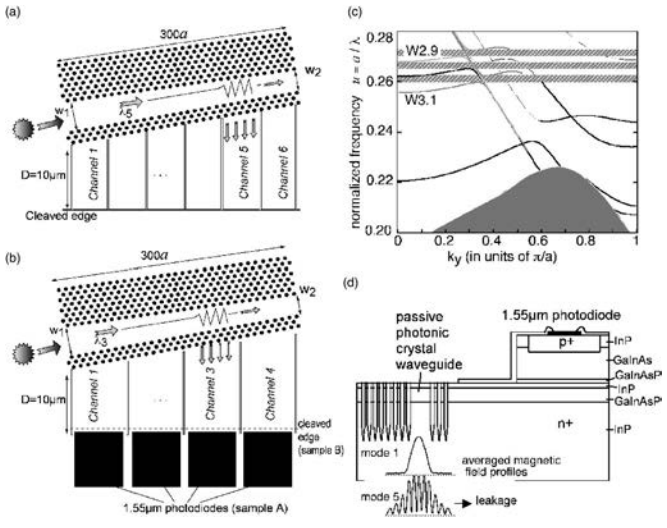

FIG. 1. (a) Scheme of sample B. The waveguide width shrinks from $w_1 = 4.1a\sqrt{3}/2$ to $w_2 = 3.9a\sqrt{3}/2$, inducing a total shift $\Delta u = 0.01$ of the mini-stop-band frequency. The six lateral channels have a $50a$ length. The fate of a particular wavelength, λ_5, is illustrated. (b) Scheme of sample A, with four integrated photodiodes. (c) Superimposed dispersion relations for photonic crystal waveguides in a InP-based heterostructure (air filling factor: 45%). The MSB shifts up between extreme widths w_1 and w_2, and is centered around $u = 0.265$ for the basic $W3^K$ A case. (d) Cross section of sample B. Note the technological challenge of deep-etching photonic crystal near photodiodes pads of 800 nm height. Mode profiles for both fundamental and fifth-order mode are depicted.

[a)]Author to whom correspondence should be addressed; electronic mail: Henri.Benisty@iota.u-psud.fr

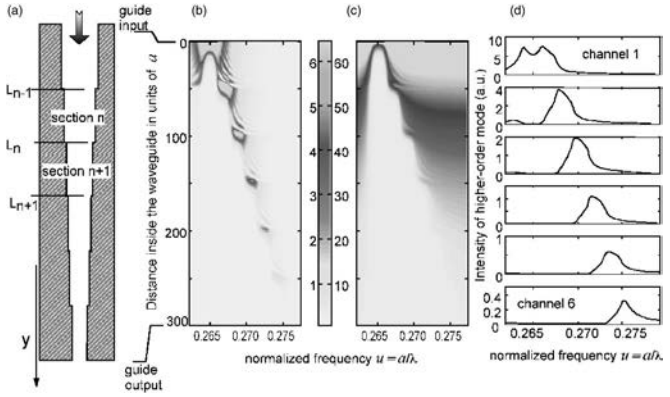

FIG. 2. (a) Scheme of a N sections waveguide; gray-level map of the simulated structure; (b) fifth-order mode intensity; (c) fundamental mode intensity as a function of the distance and frequency, using actual loss data; and (d) intensity spectra integrated over each section length.

pling section. In this section, the fundamental mode is coupled to the higher order mode, which has a slower group velocity and a much deeper penetration in the photonic crystal cladding. Thinning one of the walls of the PXCW down to a few rows, this mode leaks out laterally [Figs. 1(a) and 1(b)]. The splitting ratio may be widely adjusted through parameters such as section length, hole diameter, etc.

In this letter, we focus on the extreme case of complete extraction. We model it based on the coupled-mode theory. We discuss first realizations and corresponding measurements by purely optical methods. A first realization with four photodiodes validates its potential for real-world integration.

Coupled mode theory is an efficient design tool for PXCW[10,11] near the MSB regions including propagation losses.[11] We apply it here to a multisection waveguide having a staircased decreasing width [Fig. 2(a)]. The scalar field in quasi-TE polarization is actually the H field.

The field $E_n(x,y)$ in the nth section of the PXCW can be written as a sum of the fundamental mode of amplitude $R_n(y)$ and a higher order mode of amplitude $S_n(y)$:

$$E_n(x,y) = R_n(y)E_n^r(x)e^{-i\beta_n^r(y-L_{n-1})} + S_n(y)E_n^s(x)e^{+i\beta_n^s(y-L_{n-1})}, \tag{1}$$

where β_n denotes the propagation constant in the nth section, E_n^r and E_n^s are the uncoupled mode profiles and $R_n(y)$ et $S_n(y)$ are solutions of the coupled equations:

$$\frac{dR_n}{dy} = -(i\delta_n^r + \alpha_n^r)R_n - i\kappa_n S_n,$$
$$\frac{dS_n}{dy} = +i\kappa_n R_n + (i\delta_n^s + \alpha_n^s)S_n. \tag{2}$$

α_n is the propagation losses, and $\delta_n=(2\pi/a)n_g(u_0-u)$ is the detuning to the Bragg condition ($u=a/\lambda$ is the normalized frequency), n_g being the group index, and a the photonic crystal period.

The coupling constant is related to the overlap of both modes (r) and (s) with the modulation. Hence with notations usual to coupled mode theory practitioners, as in Ref. 11:

$$\kappa_n = \frac{\kappa_n^2}{4\beta_n}\int_{-\infty}^{+\infty} g_1^n(x)E_n^r(x)E_n^{s^*}(x)dx \tag{3}$$

save for the section-related subscript n. Continuity at $y=L_n$ gives for example for the (r) mode:

$$R_n(y=L_n)\exp(i\beta_n^r(L_n-L_{n-1}) = R_n(y=L_n) \tag{4}$$

while we take $R_1(y=0)=1$ and $S_N(y=L_N)=0$. We assume uniform propagation losses ($\alpha_{n-1}^r=\alpha_n^r$ and $\alpha_{n-1}^s=\alpha_n^s$), consistent with a spectral shift of the MSB of a few percent.

The anticrossing exploited here is that of a so-called $W3^K$ A waveguide in a triangular photonic crystal lattice of air holes of local period a (three missing rows, row-to-row distance of $4(\sqrt{3}a/2)$ at holes centers). The simulated device has six sections of equal length, $50a$ [Fig. 1(a)]. The choice of a staircased device clarifies phenomena related to crosstalk, and is also unavoidable in practice considering the unit step of a few nm of the current e-beam definition tools. The simulated width varies between $W3.1^K$ A and $W2.9^K$ A, corresponding to a 5% variation. The group index n_g for each mode (r,s) are obtained from the dispersion relation computed with the supercell approach.[12] For a 2D photonic crystal etched through a vertical InP-based heterostructure, the matrix index is taken as the effective index of the underlying waveguide $n_{\text{eff}}=3.21$. For an air-filling factor of 35%, we find: $n_{gr}=3.21$, for the fundamental mode (r), and $n_{gs}=48$ for the fifth order mode (s), neglecting material dispersion. The MSB central position shifts typically by 0.65% per section (10 nm at $\lambda=1550$ nm). The coupling constant, deduced experimentally,[11] is typically $\kappa=0.16a^{-1}$, an apparently high value intimately related to the low group velocity of mode (s). Propagation losses of each mode are also deduced from measurements[11]: $\alpha_r=135\ \text{cm}^{-1}$ and $\alpha_s=1890\ \text{cm}^{-1}$.

Figures 2(b) and 2(c) presents the simulated map of the fifth order mode intensity in a $W3^K$ A-based wedged waveguide, as a function of $u=a/\lambda$ and distance y along the device. Figure 2(d) presents the section-wise integrated intensity spectra for this mode. The fifth-order mode is generated in each section at a different MSB frequency. The map reveals some crosstalk between each channel in this raw design: for the present proof-of-principle simulation, the crosstalk is found to be −3 dB. By optimizing the design, it can easily go down to −15 to −20 dB, as required in C-WDM networks for wavelength monitoring purpose.

Two samples, denoted A and B, were fabricated onto two different InP-based heterostructures. Sample A has on top of the guide a p-n junction to integrate the photodiodes through evanescent mode coupling [Figs. 1(b) and 1(d)].[13] The other (B) has its waveguide loaded with absorbing quantum wells, in order to provide internal probe light for physical measurement purpose, by collecting the "sieved" light beams sideways at a cleaved edge instead of feeding a photodiode.[12] Six lateral output channels are defined along the waveguide axis [Fig. 1(a)]. The photonic crystal of sample B is fabricated by using inductively coupled plasma reactive-ion etching.[14] For case A, the photonic crystal structures are fabricated in recessed areas aside the photodiodes mesa, using chemically assisted ion beam etching.[15] In order to ensure a large lateral signal level rather than spectral selectivity, only four photodiodes were defined in the same total length. The photonic crystal period is $a=400$ nm for sample A (420 nm for sample B) and the air filling factor is $f=35\%$ for both. The device is

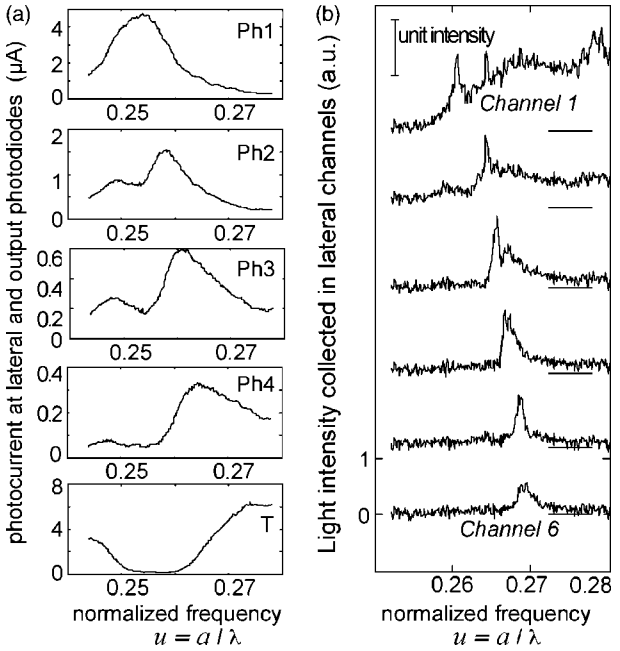

FIG. 3. (a) Experimental spectra of photocurrents in the four photodiodes Ph1,…,Ph4 lying on the thinned side of the 300*a* long $W3^K$ waveguide, and for the photodiode *T* monitoring the guide end and (b) experimental spectra of the intensities collected at the six lateral channels of the 300*a* long $W3^K$ waveguide. Excess signals at $u>0.264$ in channel 1 is stray light from the nearby laser spot, not going through the device.

a $W3^K$ A-based waveguide, with a total width variation identical to simulations. Similar results were obtained for $W5^K$ A-based guide.

Sample A was measured using a conventional end-fire technique. A tunable laser source [(1460−1660 nm)/−3 dBm] fed light through a microlensed, polarization-maintaining fiber into a ridge waveguide of width similar to the PXCW. The four photodiodes signals Ph1,…,Ph4 are in the 0.5–5 μA range, easily measured by lock-in detection. For transmission measurements, another photodiode "*T*" was also implemented at the output of the PXCW. The corresponding spectra for a $W3^K$ A-based guide are shown on Fig. 3(a). The output photodiode spectrum (*T*) exhibits a wide region of very low transmission around a normalized frequency $u=0.26$. This corresponds to the overlap of all local MSBs. Lateral photodiodes exhibit a peak around the MSB wavelength of the corresponding waveguide section. The wavelength of the MSB here $\Delta\lambda=50$ nm, a value adapted to C-WDM networks. Propagation losses of the fundamental mode can be deduced from the decay spans along the PXCW. We find $\alpha_r=150\ \mathrm{cm}^{-1}$, in good agreement with reported values:[16] integration of photodiodes near photonic crystal is feasible without altering the photonic crystal properties. The measured quality factor is 25, in good agreement with the expected value related to the MSB width. One can also notice that the peaks are asymmetrical. As the higher-order mode propagates backward in the waveguide, part of this mode created in channel *n* leaks through channel $n-1$, as a lower wavelength contribution in this latter channel [see Fig. 2(b)]. Finally, from the spectral shape of the signal in *T* [Fig. 3(a)], the relative extinction ratio for the extracted wavelengths is 20 and insertion losses are about −3 dB.

A spectrally resolved set of optical data was obtained using sample B, with excitation at the guide entrance and collection at a cleaved edge, and TE polarized collection, as practiced for other complex structures.[17] The advantage is that only the etching step is needed. Spatial resolution results in better spectral resolution, for reasons to be investigated in depth yet. The spectra for the same $W3^K$ A-based wedged PXCW are shown on Fig. 3(b). The overall results are very comparable to that obtained with the heterostructure A: a shifting, asymmetrical peak clearly shows up. Thanks to the finer spectral resolution, the measured quality factor reaches $Q=300$ at $\lambda=1.55$ μm, which converts into a channel interspacing of 550 GHz, already suited to C-WDM.

In conclusion, we have simulated and characterized a very compact photonic crystal integrated wavelength monitor toward C-WDM applications. The polarization issue is not addressed here. In its present state, this principle could be used to monitor the wavelength emitted by a laser or a laser array in a monolithic manner. Further engineering will target devices for C-WDM photonic integrated circuits. Primary trends are: (i) monitored wavelengths are chosen by adjusting the width of the waveguide and/or the filling factor of the photonic crystal; (ii) crosstalk can be limited by controlling backward propagation of the higher-order mode; (iii) the relative amount of laterally extracted power can be adjusted by varying the width of the wall; and finally, (iv) the number and lengths of the different sections can be chosen as desired.

[1] B. Mason, S. P. DenBaars, and L. A. Coldren, IEEE Photonics Technol. Lett. **10**, 1085 (1998).
[2] M. K. Smit and C. v. Dam, IEEE J. Sel. Top. Quantum Electron. **2**, 236 (1996).
[3] M. Strassner, C. Luber, A. Tarraf, and N. Chitica, IEEE Photonics Technol. Lett. **14**, 1548–1550 (2002).
[4] B. Vanderhaegen, D. V. Tourhout, J. D. Merlier, G. Starlet, L. V. Wassenhove, I. Moerman, P. V. Daele, R. Baets, X. J. M. Leitens, J. W. M. v. Uffelen, and M. K. Smit, *Proceedings of the 9th European Conference on Integrated Optics*, Torino, Italy, 1999, p. 381.
[5] S. Olivier, C. Weisbuch, and H. Benisty, Opt. Lett. **28**, 2246 (2003).
[6] C. Cuisin, G. H. Duan, J.-P. Chandouineau, O. Drisse, F. Gaborit, S. Hubert, L. Legouézigou, O. Legouézigou, F. Pommereau, F. Poingt, N. Bouché, and B. Thedrez, *ECOC 2003*, Rimini, Italy, 2003, Paper Tu 3.1.3.
[7] T. Happ, M. Kamp, A. Forchel, J.-L. Gentner, and L. Goldstein, Appl. Phys. Lett. **82**, 4 (2003).
[8] S. Olivier, M. Rattier, H. Benisty, C. J. M. Smith, R. M. D. L. Rue, T. F. Krauss, U. Oesterle, R. Houdré, and C. Weisbuch, Phys. Rev. B **63**, 113311 (2001).
[9] S. Olivier, H. Benisty, C. J. M. Smith, M. Rattier, C. Weisbuch, and T. F. Krauss, Opt. Quantum Electron. **34**, 171 (2002).
[10] H. Kogelnik and C. V. Shank, J. Appl. Phys. **43**, 2327 (1972).
[11] S. Olivier, H. Benisty, C. Weisbuch, C. J. M. Smith, T. F. Krauss, and R. Houdré, Opt. Express **11**, 1490 (2003).
[12] H. Benisty, C. Weisbuch, D. Labilloy, M. Rattier, C. J. M. Smith, T. F. Krauss, R. M. D. L. Rue, R. Houdré, U. Oesterle, and D. Cassagne, IEEE J. Lightwave Technol. **17**, 2063 (1999).
[13] A. Umbach, D. Trommer, G. G. Mekonnen, and G. Unterborsch, Electron. Lett. **32**, 2143 (1996).
[14] F. Pommereau, L. Legouézigou, S. Hubert, S. Sainson, J.-P. Chandouineau, S. Fabre, G.-H. Duan, B. Lombardet, R. Ferrini, and R. Houdré, J. Appl. Phys. **95**, 2242 (2004).
[15] S. Golka, K. Janiak, H. J. Hensel, H. Heidrich, E. Schwoob, and H. Benisty, *Proceedings of the 15th Indium Phosphide and Related Materials Conference*, Santa Barbara, CA, 2003, p. 75, paper TUA 2.5.
[16] M. V. Kotlyar, T. Karle, D. Settler, L. O'Faolain, and T. F. Krauss, Appl. Phys. Lett. **84**, 3588 (2004).
[17] C. J. M. Smith, R. M. De La Rue, M. Rattier, S. Olivier, H. Benisty, C. Weisbuch, T. F. Krauss, R. Houdré, and U. Oesterle, Appl. Phys. Lett. **78**, 1487 (2001).